The Optical Rotatory Power of Water

Christine Isborn,* Kacey Claborn,* and Bart Kahr*

Department of Chemistry, University of Washington, Box 351700, Seattle, Washington 98195-1700

Received: May 5, 2007

Ab initio molecular orbital calculations of the optical rotatory response of a single oriented water molecule are described. The unique tensor element $\mathcal{G}_{xy}$ was computed to be −0.047 bohr^3 with CCSD/6-311+G(d,p). A value of −0.033 was obtained with the minimal valence basis that was better suited to parsing the rotatory response among a limited number of excited states. Transition moments were calculated ab initio and qualitatively derived from the wave functions. Rotations were reckoned from the relative dispositions of the transition moments with respect to the wavevectors. In this way, it was possible to intuitively reckon the form of the optical rotation tensor consistent with that from higher levels of theory and to establish which excitations make the most significant contributions.

1. Introduction

Only during the past decade have the vexing obstacles to computing optical rotation (OR) of molecules from first principles begun to yield to successive advancements in quantum chemistry.[1] The smallest familiar chiral molecule, C_2-symmetric H_2O_2, has been the emphasis of a number of theoretical investigations of OR.[2,3] However, H_2O_2 is not the simplest naturally optically rotatory compound; H_2O is simpler still. Reflecting upon the OR of H_2O is valuable because there can be no faithful explanation of OR without a grasp of molecular electronic structure, and even beginners can construct the qualitative molecular orbitals of H_2O. For this reason, H_2O is an entrée to a structure-based interpretation of OR and its orientational dependence. Here, we compute the OR tensor for an oriented water molecule and analyze contributions from individual states.

OR of achiral H_2O may be counterintuitive to some because the necessary condition for OR remains widely misunderstood among chemists.[4] Enantiomorphism is often cited in organic chemistry textbooks as the necessary condition for optical activity. We now recognize, however, that the point group D_{2d},[5] and its achiral subgroups S_4,[6] C_{2v},[7] and C_s,[8] are compatible with OR in some directions with respect to oriented molecules; measurements of the OR tensors for non-enantiomorphous compounds have been achieved in crystals.[5−9] The OR of achiral molecules averaged over all orientations must be zero, but this does not exclude H_2O or other achiral molecules[10] from theoretical chiroptical inquiries. Barron's comprehensive treatment of OR[11] includes a cartoon indicating the rotation of a polarized wave striking a water molecule in a general direction, but the details of this interaction have not heretofore been presented.

In an effort to give a simple explanation of OR on the basis of molecular electronic structure, while emphasizing the necessary condition for OR, we carried out ab initio computations of the OR of the water molecule, the simplest familiar optically rotatory compound. We show that, for the water molecule, a minimal valence calculation captures the OR response achieved at a higher level of theory. We then parsed the response with the minimal basis into all contributing excitations. By visualizing the molecular orbitals, we can graph the transition moments with respect to the molecular coordinate system. These moments are then coupled together to give the OR response. We anticipate that a qualitative interpretation of the OR tensor in terms of molecular electronic structure will be useful in establishing chiroptical structure/property relationships.

The expression of the symmetric OR tensor for oriented molecules was derived by Buckingham and Dunn[12]

$$\mathcal{G}_{\alpha\beta} = -\frac{1}{2}\left[G'_{\alpha\beta} + G'_{\beta\alpha} - \frac{1}{3}\omega(\epsilon_{\alpha\gamma\delta}A_{\gamma\delta\beta} + \epsilon_{\beta\gamma\delta}A_{\gamma\delta\alpha})\right] \quad (1)$$

where $G'_{\alpha\beta}$ is the electric dipole−magnetic dipole polarizability, the trace of which contributes to OR in isotropic systems, ω is the frequency of light, ϵ is the Levi−Civita operator, and $A_{\alpha\beta\gamma}$ is the electric dipole−electric quadrupole polarizability, which averages to zero for isotropic media. The polarizability linear response tensors are defined as

$$G'_{\alpha\beta} = -i\langle\langle \mu_\alpha; m_\beta \rangle\rangle = -2\omega \sum_n \mathrm{Im}\frac{\langle\psi_0|\mu_\alpha|\psi_n\rangle\langle\psi_n|m_\beta|\psi\rangle}{\omega_{0n}^2 - \omega^2} \quad (2)$$

$$A_{\alpha\beta\gamma} = -\langle\langle \mu_\alpha; \Theta_{\beta\gamma} \rangle\rangle = 2\sum_n \omega_{n0}\frac{\langle\psi_0|\mu_\alpha|\psi_n\rangle\langle\psi_n|\Theta_{\beta\gamma}|\psi_0\rangle}{\omega_{0n}^2 - \omega^2} \quad (3)$$

where μ, m, and Θ are the electric dipole, magnetic dipole, and Buckingham's traceless electric quadrupole operators, respectively, summed over all electrons i and given in atomic units as

$$\mu_\alpha = -\sum_i r_{i\alpha} \quad (4)$$

$$m_\alpha = -\frac{1}{2}\sum_i l_{i\alpha} \quad (5)$$

$$\Theta_{\alpha\beta} = -\frac{1}{2}\sum_i (3r_{i\alpha}r_{i\beta} - r_i^2\delta_{\alpha\beta}) \quad (6)$$

The form of the Buckingham−Dunn equation (eq 1) differs from the original by a factor of i. To be consistent with the linear

* Corresponding author. E-mail: cisborn@u.washington.edu (C.I.); kaceycla@u.washington.edu (K.C.); kahr@chem.washington.edu (B.K.).

10.1021/jp073439n CCC: $37.00
Published on Web 07/13/2007

response literature, we instead include the i in the definition of the G' tensor (eq 2) so that only real terms enter into eq 1. Individual tensor elements of $A_{\alpha\beta\gamma}$ and $G'_{\alpha\beta}$ depend on the choice of gauge origin, but the Buckingham−Dunn tensor is origin-independent (translationally invariant) in a complete basis because of cancellation from the origin dependent terms.[13] The optical rotation tensor $\mathcal{G}$ calculated with the equations above has units of bohr^3. To compare the calculated value to an experimental measurement (were one available), we require the experimental number density N: $\phi((radians)/(length)) = 2\pi\mathcal{G}N(\omega/c)$.

The sum over all states expressions for $G'_{\alpha\beta}$ and $A_{\alpha\beta\gamma}$ come from the perturbation theory calculation of the induced dipole moment that governs molecular scattering

$$\mu_\alpha = \mu_\alpha^0 + \alpha_{\alpha\alpha'}E_{\alpha'} + \frac{1}{3}A_{\alpha\alpha'\beta'}E_{\alpha'\beta'} + \frac{1}{\omega}G_{\alpha\alpha'}\dot{B}_{\alpha'} + \ldots \quad (7)$$

where $E_{\alpha'}$ is the electric field in direction α', $E_{\alpha'\beta'}$ is the electric field gradient along β', $\dot{B}_{\alpha'}$ is the time derivative of the magnetic field along α', $\alpha_{\alpha\alpha'}$ is the usual electric dipole−electric dipole polarizability, and primed indices indicate the Einstein convention. In the above expression, the spatial dependence of the electric field is included, resulting in the omission of all but the first two terms for derivations performed within the dipole approximation. Just as the $\alpha_{\alpha\alpha'}$ tensor describes how the electron density will respond to a linear electric field, the $A_{\alpha\beta\gamma}$ and $G'_{\alpha\beta}$ tensors describe how the electron density will respond to an electric-field gradient and time-varying magnetic field, respectively.

These last two terms give rise to the part of the induced dipole moment that is oscillating 90° out of phase with the incident electric field. Forward scattering from a 2D sheet of molecules yields an additional 90° phase shift.[14] These phase shifts cancel, giving a plane wave front that is in phase with the incident electric field. This results in scattered radiation that is in phase with the incident field, but with an orthogonal polarization component, leading to an overall azimuthal rotation of the plane of the electric field vector.

2. Computational Details

To develop a practical understanding of OR on the basis of analysis of contributions from all possible transitions, we must have a manageable number of transitions. For water, with a minimal STO-3G basis, there are only eight transitions. Optical properties, however, vary with both the choice of basis set and the treatment of correlation. We thus compare our frequency-dependent minimal valence basis STO-3G Hartree−Fock (HF),[15] also known as coupled perturbed Hartree−Fock or the random phase approximation, calculations of the OR tensor to higher-level calculations, all computed with the DALTON[16] program. With the HF/STO-3G level of theory, transition moments were computed as single residues of the linear response function.[17] To test the effects of electron correlation, we performed frequency-dependent linear response theory calculations using the gradient-corrected hybrid B3LYP density functional[18] and the coupled-cluster singles and doubles (CCSD) levels of theory.[19] The frequency used was the sodium-D wavelength of light (ω = 0.0773 atomic units = 589 nm). Results are given for several basis sets, ranging from STO-3G (7 basis functions) to 6-311+G* (28 basis functions).

The rationale for the high-level calculations was naturally to compute accurate quantities. The minimal valence basis was instructive in decomposing the OR into contributions from comparatively few electronic transitions[20] so as to develop an intuitive sense of the sign and magnitude of the OR tensor. We give a pictoral representation of the coupling of the transition moments to form the OR tensor and show how their relative orientations with respect to the incident light wavevector determines the sign of the OR. In the calculations, the center of mass was chosen as the gauge origin, and the H_2O geometry[21] was optimized at the B3LYP/cc-pVTZ level of theory in Gaussian03.[22]

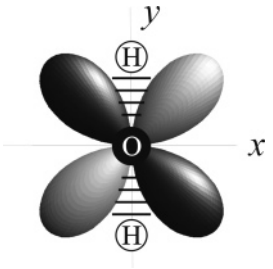

Figure 1. Representation surface of the optical rotation tensor of H_2O. A negative OR value (levorotation) is calculated for $\mathcal{G}_{xy}$ for all levels of theory. Light = levorotation, dark = dextrorotation.

TABLE 1: Optical Rotation for Water by Symmetry Contributions[a]

	contribution by symmetry			
method	$\mathcal{G}_{xy}(B_1)$	$\mathcal{G}_{xy}(B_2)$	$\mathcal{G}_{xy}(A_1)$	sum $\mathcal{G}_{xy}$
HF/STO-3G	0.0090	−0.1127	0.0706	−0.0330
HF/6-31+G*	−0.0102	−0.0993	0.0964	−0.0130
HF/6-31++G	−0.0048	−0.1274	0.1194	−0.0128
HF/6-311+G*	−0.0055	−0.1219	0.1150	−0.0124
B3LYP/STO-3G	0.0108	−0.1097	0.0698	−0.0291
B3LYP/6-31+G*	−0.0105	−0.1048	0.1040	−0.0114
B3LYP/6-31++G	−0.0098	−0.1384	0.1318	−0.0164
B3LYP/6-311+G*	−0.0073	−0.1308	0.1243	−0.0139
CCSD/STO-3G	0.0211	−0.1338	0.0686	−0.0440
CCSD/6-31+G*	−0.0110	−0.1329	0.1014	−0.0425
CCSD/6-311+G*	−0.0041	−0.1643	0.1212	−0.0471

[a] Calculated at the frequency of the sodium D line = 589 nm.

3. Results and Discussion

There is only one independent OR tensor element ($\mathcal{G}_{xy} = \mathcal{G}_{yx}$) for C_{2v} H_2O. This single value fixes the tensor eigenvalues (maximum OR magnitude) between the x and y axes of the molecule (Figure 1). A negative $\mathcal{G}_{xy}$ indicates negative optical rotation for wavevectors in the $[x,y]$ and $[-x,-y]$ directions. The OR is divided into contributions from transitions of various symmetries as shown in Table 1. These are calculated from the Buckingham−Dunn equation as

$$\mathcal{G}_{xy} = -\frac{1}{2}\left[G'_{xy} + G'_{yx} - \frac{1}{3}\omega(A_{yyz} - A_{zyy} - A_{xxz} + A_{zxx})\right] \quad (8)$$

$$\mathcal{G}_{xy}(B_1) = -\frac{1}{2}\left[G'_{xy} - \frac{1}{3}\omega(-A_{xxz})\right] \quad (9)$$

$$\mathcal{G}_{xy}(B_2) = -\frac{1}{2}\left[G'_{yx} - \frac{1}{3}\omega(-A_{yyz})\right] \quad (10)$$

$$\mathcal{G}_{xy}(A_1) = -\frac{1}{2}\left[-\frac{1}{3}\omega\,(-A_{zyy} + A_{zxx})\right] \quad (11)$$

Comparing the optical rotation from different methods and basis sets, we see that for the B_2, A_1, and summed contributions to $\mathcal{G}_{xy}$, the HF/STO-3G results have the same sign and order of magnitude as for the higher levels of theory. For all methods, the B_1 contribution is very small and changes from positive to negative for any basis set larger than STO-3G. In the minimal

TABLE 2: Optical Rotation (OR) of H_2O Excitations[a]

transition symmetry	MO excitations (and corresponding coefficients)	μ	m	Θ	$\mathcal{G}_{xy}$
$1B_1$	$5 \rightarrow 6$ (0.68)	−0.10 (x)	−0.50 (y)	0.06 (xz)	0.009
$1A_2$	$5 \rightarrow 7$ (0.69)	0	−0.68 (z)	−0.11 (xy)	0.000
$1A_1$	$3 \rightarrow 7$ (0.18) $4 \rightarrow 6$ (0.67)	−0.40 (z)	0	−0.31 (xx), 0.51 (yy)	0.014
$1B_2$	$3 \rightarrow 6$ (0.29) $4 \rightarrow 7$ (0.61)	0.34 (y)	−0.75 (x)	−0.11 (yz)	−0.022
$2B_2$	$3 \rightarrow 6$ (0.61) $4 \rightarrow 7$ (−0.28)	1.40 (y)	−0.09 (x)	−1.77 (yz)	−0.088
$2A_1$	$2 \rightarrow 6$ (−0.16) $3 \rightarrow 7$ (0.64) $4 \rightarrow 6$ (−0.12)	0.89 (z)		0.98 (xx), −1.23 (yy)	0.049
$3A_1$	$2 \rightarrow 6$ (0.67)	−0.23 (z)	0	−0.89(xx), 0.88 (yy)	0.007
$3B_2$	$2 \rightarrow 7$ (0.69)	0.14 (y)	−0.15 (x)	−1.09 (yz)	−0.003
SUM					−0.033

[a] Computed at the HF/STO-3G level of theory.

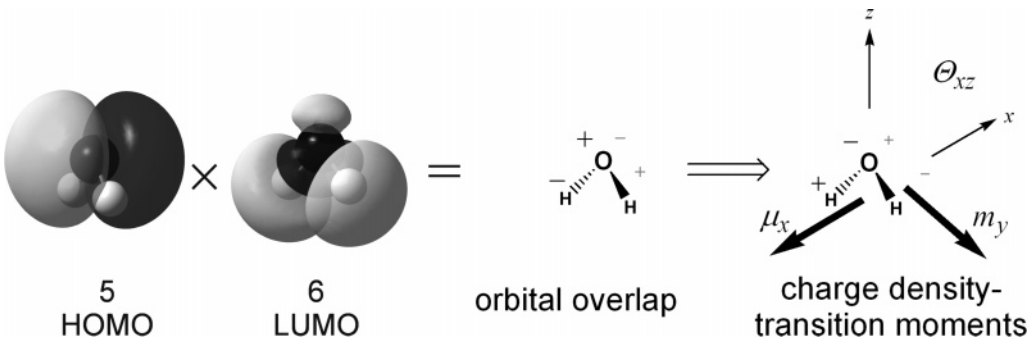

Figure 2. HOMO−LUMO transition of symmetry B_1. Signs (±) indicate regions of orbital overlap (center) and charge build-up and depletion (right). Transition moments created are an electric dipole moment along $-x$, an electric quadrupole in the xz plane, and a magnetic dipole along $-y$.

basis set, the only B_1 transition is from the HOMO to the LUMO. Larger basis sets allow for more flexibility of charge rearrangement in the B_1 states, changing the sign of the contributions to OR. The B_2 contributions are negative and the A_1 contributions are positive, but the B_2 contribution is larger for all methods studied, and so the sign of the OR from the B_2 transitions determines the sign of the overall response. Larger basis sets increase the magnitude of both the A_1 and B_2 transitions. Electron correlation favors the B_2 transitions over A_1, as the larger basis set CCSD calculations of $\mathcal{G}_{xy}$ are three times as large as the Hartree−Fock values.

We proceed from computed tensor elements to an understanding of the rotatory response by developing an intuition for the transition moments that make up the tensors. In the Buckingham−Dunn equation, the perturbation theory G' and A tensors are formed from summing over all excited states. It is the relative orientation of these moments that governs the sign of the OR. With a minimal basis, we can relate the calculated OR tensor value to the transition moments for each excitation, as seen in Table 2. With Snatzke's qualitative molecular orbital (MO) analysis, in which the initial and final molecular orbitals of the transition are multiplied pictorially,[23] we can reconcile the orientation and magnitude of the transition moments with the electronic structure of the molecule.

H_2O has the following configuration: $(1a_1)^2(2a_1)^2(1b_2)^2(3a_1)^2(1b_1)^2(4a_1)^0(2b_2)^0$. Electric dipole allowed excited-state symmetries of a C_{2v} molecule are A_1, B_1, and B_2. The A_2 transitions are not electric dipole allowed and they do not contribute to OR. Analysis of the minimal basis state-by-state contributions to the OR tensor show that all the A_1 and B_1 transitions make contributions (Table 1) that oppose those of the B_2 transitions. For larger basis sets, the sign of the total B_1 contribution changes sign, indicating that these transitions can be either positive or negative. It is, however, a small contributor, even with the larger basis sets. The sign of the overall OR tensor is determined by the dominant B_2 transitions.

According to the Snatzke method (Figure 2), the $1B_1$ transition is formed from the product of the highest occupied MO (HOMO), the lone electron pair containing a p_x orbital on oxygen, with the lowest unoccupied MO (LUMO), the p_z orbital on oxygen mixing with the in-phase combination of hydrogen orbitals. The positive and negative orbital overlap, localized on the oxygen p-like orbitals, corresponds to regions of negative charge accumulation and depletion, respectively. The charge build-up during the transition leads to μ along $-x$, and Θ in the xz plane. The transition magnetic dipole moment (m) is established by turning the occupied orbital into the unoccupied orbital so as to maximize overlap most efficiently. This gives the motion of electrons and thus the magnetic moment by the left hand rule. Because the μ_x transition moments from B_1 symmetry excitations result only from overlap of the p_x lone pair orbital on oxygen with other orbitals, the orbital overlap does not extend very far in space. This leads to a relatively small magnitude for μ_x and, despite a relatively large transition magnetic dipole moment, B_1 transitions having a small overall contribution to the OR tensor (Figure 3).

In a chiral molecule, components of these transition moments are parallel (dextrorotation) or antiparallel (levorotation), whereas in a C_{2v} achiral molecule, they are orthogonal. Thus, for achiral molecules such as water, with perpendicular moments, it is the direction of the wavevector that determines the sign of OR. For the B_1 transitions of water (Figure 3), transition moments projected onto the $[x,y]$ or $[-x,-y]$ wavevector are parallel, giving rise to dextrorotation (dark lobes of tensor), whereas projection onto the $[x,-y]$ or $[-x,y]$ wavevectors gives antiparallel moments and levorotation (light lobes of tensor).

The B_2 transition moments can be established from the MOs likewise with μ along y, m along $-x$, and Θ in the yz plane. B_2

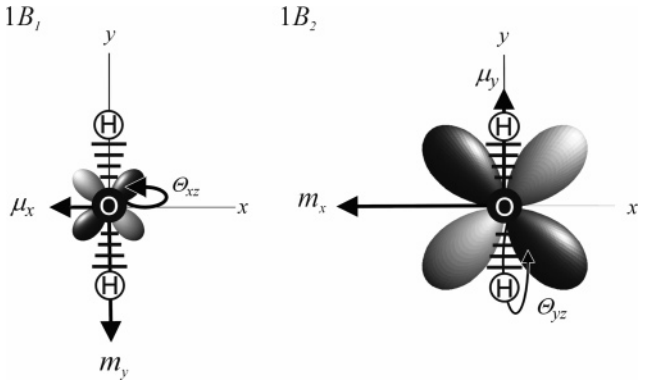

Figure 3. Relevant transition moments (μ, m, and Θ) and corresponding OR tensor for the $1B_1$ and $1B_2$ transitions as calculated in Table 2. The transition moments and tensors were scaled to reflect their relative magnitudes as given in Table 2.

excitations yield an electric dipole transition moment along the *y*-axis from electron density moving from one hydrogen to the other (Figure 4a). This leads to a larger electric dipole transition moment than in B_1 transitions, and to a larger OR tensor. Figure 3 shows how the relative orientation of the B_2 transition moments leads to OR contributions of opposite sign from those of B_1 symmetry and how the larger magnitude of the B_2 moments also yields a larger OR tensor.

A_1 transitions are distinct from B_1 and B_2 transitions in that $m = 0$, whereas the Θ values are linear and perpendicular to μ_z (Figure 4b). The diagonal elements of Buckingham's traceless Θ form of the quadrupole operator take into account contributions from each of the Cartesian directions. For example, $\Theta_{xx} = -1/2\sum_i(2r_{xi}^2 - r_{yi}^2 - r_{zi}^2)$. For all of the A_1 transitions, both of the second moments, $Q_{xx} = -\sum_i r_{xi}^2$ and $Q_{yy} = -\sum_i r_{yi}^2$, have the same sign. The transition moments Θ_{xx} and Θ_{yy}, however, have opposite signs. This occurs when one second moment Q is at least twice as large as the other. For the A_1 transitions of water, Q_{yy} is more than five times as large as Q_{xx}. Thus, the opposite signs of Θ_{xx} and Θ_{yy} show the great asymmetry between the *x* and *y* directions of water. Although the transition moments Θ_{xx} and Θ_{yy} have opposite signs, the A_{zxx} and A_{zyy} contributions to the OR response also enter into the Buckingham−Dunn equation (eq 8) with opposite signs. Thus, A_{zxx} and A_{zyy} give OR of the same sign (positive). This only occurs because of the large magnitude of Q_{yy} in comparison to Q_{xx}. If there were no asymmetry in the *x* and *y* directions, Θ_{xx} and Θ_{yy} would have the same sign and magnitude, and thus A_{zxx} and A_{zyy} would cancel in the Buckingham−Dunn equation. As in the B_2 transitions, the extension of the molecule along the *y* direction creates a larger electronic response along *y* than along *x*; however, in the A_1 case, the transitions create positive rather than negative OR.

Contributions from A_1 transitions, lacking magnetic dipole transition moments, cannot be determined from the scalar product of μ and m projected on the wave vector of light. We find that a positive product of Q_{xx} and μ_z yields dextrotation for the wave vector in the [*x*,*y*] quadrant, whereas a positive product of Q_{yy} and μ_z yields levorotation for the wave vector in the [*x*,*y*] quadrant. For water, both products are always negative, but Q_{yy} is much larger than Q_{xx}, so that all of the A_1 transitions produce dextrorotation.

The intuition we developed regarding the OR of water can be applied to formaldehyde, likewise of C_{2v} symmetry. Formaldehyde extends further along *z* (adding nuclei) and along *x* (adding the CO π system). The π system allows for much greater rotation in the *xz* plane for the B_1 transitions. In water, the hydrogen atoms in the lower half of the molecule dominate the response along *y* and *z*. Only the lone pair on oxygen is active in the *x* direction. In formaldehyde, the oxygen on the upper half of the molecule plays a large role in the response, which can switch the relative orientation of the μ and m transition moments, and thus the sign of the OR.

4. Conclusions

At both the low and high levels of theory, the B_2 transitions of water produce levorotation for wavevectors in the [*x*,*y*] and

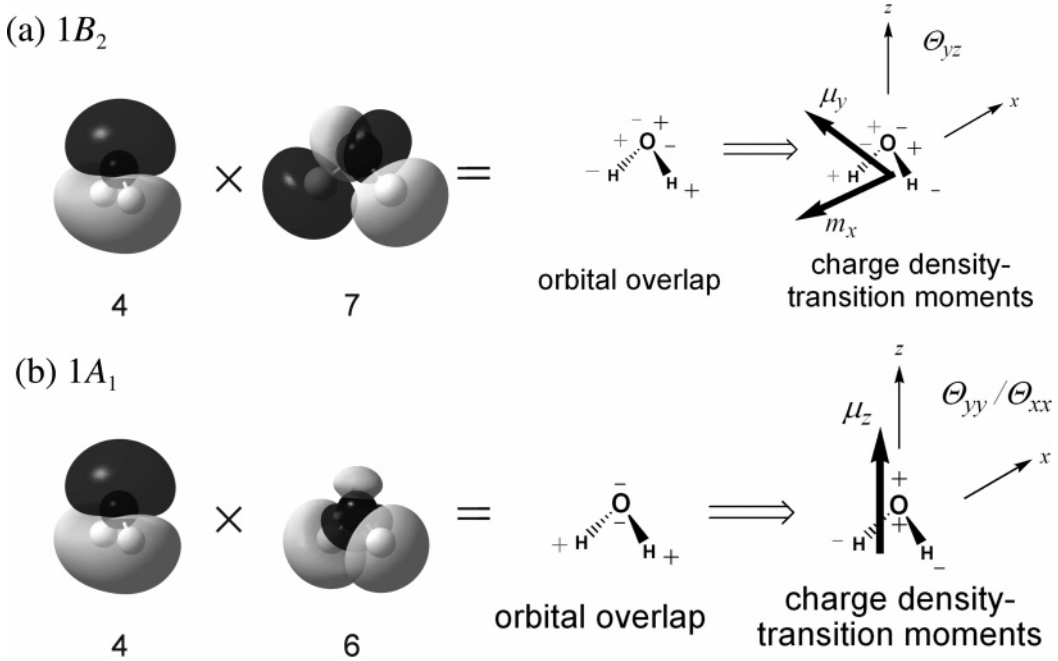

Figure 4. (a) Overlap for MOs 4 and 7 that contribute to transition $1B_2$. Signs (±) indicate regions of orbital overlap (center) and charge build-up and depletion (right). Transition moments include an electric dipole moment along *y*, an electric quadrupole in the *yz* plane, and a magnetic dipole along $-x$. (b) The overlap for MOs 4 and 6 that contribute to transition $1A_1$. Signs (±) indicate regions of orbital overlap (center) and charge build-up and depletion (right). Transition moments include an electric dipole moment along *z*, and two linear electric quadrupole moments.

$[-x,-y]$ quadrants, whereas the A_1 transitions produce dextrorotation. The B_2 transitions, however, have their transition dipole moment along the bonds of the molecule, leading to a larger transition dipole moment in this direction and thus they dominate the overall sign of the OR. The molecular orbital and transition moment analysis of the OR of a single, oriented achiral molecule as provided here is insightful, because, given the simplicity of the electronic structure of H_2O, any chemist can derive its wave functions and transition moments qualitatively. Thus, the results of the ab initio computations that are often opaque can be rendered on the blackboard.

Can we put our computations to the test of experiment? The simplest way to orient water molecules is to grow ice. Of the 12 known ice phases, only the ordered hexagonal phase XI (space group $Cmc2_1$, point symmetry C_{2v}) has a symmetry compatible with OR.[24,25] Ice XI is thought to exist on the planetoid Pluto.[26] It can be grown at 70 K and ambient pressure on planet Earth.[27] We aspire to measure the optical rotatory power of ice XI using recent advances in OR imaging.[28] The intuition developed here for the OR for a single oriented water molecule will undoubtedly require modification in extension to water clusters where intermolecular interactions play a large role in the electronic response. By comparing single molecule calculations to those in the aggregate, we will learn more about the intermolecular contributions to optical activity.

Acknowledgment. This work was supported by the U.S. National Science Foundation. We are grateful to K. Ruud for assistance.

References and Notes

(1) (a) Polavarapu, P. L. *Mol. Phys*. **1997**, *91*, 551−554. (b) Kondru, R. K.; Wipf, P.; Beratan, D. N. *Science* **1998**, *282*, 2247−2250. (c) Yabana, K.; Bertsch, G. F. *Phys. Rev. A* **1999**, *60*, 1271−1279. (d) Stephens, P. J.; Devlin, F. J.; Cheeseman, J. R.; Frisch, M. J. *J. Phys. Chem. A* **2001**, *105*, 5356−5371. (e) Polavarapu, P. L. *Chirality* **2002**, *14*, 768−781. (f) Stephens, P. J.; Devlin, F. J.; Cheeseman, J. R.; Drisch, M. J.; Bortolini, O.; Besse, P. *Chirality* **2003**, *15*, S57−S64. (g) Stephens, P. J.; McCann, D. M.; Cheeseman, J. R.; Frisch, M. J. *Chirality* **2005**, *17*, S52−S64. (h) Pecul, M.; Ruud, K. *Adv. Quantum Chem*. **2005**, *50*, 185−212. (i) Crawford, T. D. *Theor. Chem. Acc*. **2006**, *115*, 227−245.

(2) (a) Polavarapu, P. L.; Chakraborty, D. K. *Chem. Phys*. **1999**, *240*, 1−8. (b) Grishanin, A. B.; Zadkov, V. N. *J. Exp. Theor. Phys.* **1999**, *89*, 669−676. (c) Ruud, K.; Helgaker, T. *Chem. Phys. Lett*. **2002**, *352*, 533−539. (d) Norman, P.; Ruud, K.; Helgaker, T. *J. Chem. Phys*. **2004**, *120*, 5027−5035.

(3) For computational rotations of chiral conformations of other small molecules, see: Wiberg, K. B.; Wang, Y.-G.; Vaccaro, P. H.; Cheeseman, J. R.; Trucks, G.; Frisch, M. *J. Phys. Chem. A* **2004**, *108*, 32−38.

(4) O' Loane, K. J. *Chem. Rev*. **1980**, *80*, 41−61.

(5) Hobden, M. V. *Nature (London*) **1967**, *216*, 678. (b) Hobden, M. V. *Acta Crystallogr., Sect. A* **1968**, *24*, 676−680.

(6) (a) Hobden, M. V. *Nature (London*) **1968**, *220*, 781. (b) Hobden, M. V. *Acta Crystallogr., Sect. A* **1969**, *25*, 633. (c) Claborn, K.; Herreros, Cedres, J.; Isborn, C.; Zoulay, A.; Weckert, E.; Kaminsky, W.; Kahr, B. *J. Am. Chem. Soc*. **2006**, *128*, 14746.

(7) (a) Kaminsky, W.; Thomas, P. A.; Glazer, A. M. *Z. Kristallogr*. **2002**, *217*, 1−7. (b) Hough, L. E.; Clark, N. A. *Phys. Rev. Lett*. **2005**, *95*, 107802.

(8) Futama, H.; Pepinsky, R. *J. Phys. Soc. Jpn*. **1962**, *17*, 725.

(9) Kaminsky, W. *Rep. Prog. Phys*. **2000**, *63*, 1575−1640.

(10) (a) Kongsted, J.; Pedersen, T. B.; Osted, A.; Hansen, A. E.; Mikkelsen, K. V.; Christiansen, O. *J. Phys. Chem. A* **2004**, *108*, 3632−3641. (b) A. E. Hansen, K. L. Bak, *J. Phys. Chem. A* **2000**, *104*, 11362−11370.

(11) Barron, L. D. *Molecular Light Scattering and Optical Activity*; Cambridge University Press: Cambridge, UK, 2004; p 27.

(12) Buckingham, A. D.; Dunn, M. B. *J. Chem. Soc. A* **1971**, 1988−1991.

(13) Krykunov, M.; Autschbach, J. *J. Chem. Phys.* **2006**, *125*, 034102.

(14) Kauzmann, W. *Quantum Chemistry*: Wiley: New York, 1957; pp 600−608.

(15) Rowe. D. J. *Rev. Mod. Phys*. **1968**, *40*, 153−166.

(16) Helgaker, T.; Jensen, H. J. A.; Jørgensen, P.; Olsen, J.; Ruud, K.; Ågren, H.; Andersen, T.; Bak, K. L.; Bakken, V.; Christiansen, O.; Dahle, P.; Dalskov, E. K.; Enevoldsen, T.; Fernandez, B.; Heiberg, H.; Hettema, H.; Jonsson, D.; Kirpekar, S.; Kobayshi, R.; Koch, H.; MIkkelsen, K. V.; Norman, P.; Packer, M. J.; Saue, T.; Taylore, P. R.; Vahtras, O. *DALTON, a Molecular Electronic Structure Program*, release 2.0; University of Rochester: Rochester, NY, 2005; see http://www.kjemi.uio.no/software/dalton/dalton.html.

(17) Linderberg, J.; Öhrn. Y. *Propagators in Quantum Chemistry*, 2nd ed.; Wiley: New York, 2004.

(18) (a) Becke. A. D. *J. Chem. Phys*. **1993**, *98*, 5648−5652. (b) Lee, C.; Yang, W.; Parr, R. G. *Phys. Rev. B* **1988**, *37*, 785−789. Linear response TD-B3LYP calculations for H_2O are given in: Cai, Z.-L.; Tozer, D. J.; Reimers, J. R. *J. Chem. Phys*. **2000**, *113*, 7084−7096.

(19) (a) Koch, H.; Jørgensen. P. *J. Chem. Phys*. **1990**, *93*, 3333−3344. (b) CCSD linear response excitation energies for H_2O are given in: Koch, H.; Jensen, H. J. A.; Jørgensen, P.; Helgaker. T. *J. Chem. Phys.* **1990**, *93*, 3345−3350.

(20) For a detailed computational analysis of the electronic structure of H_2O, see: del Puerto, M. L.; Tiago, M. L.; Vasiliev, I.; Chelikowsky, J. R. *Phys. Rev. A* **2005**, *72*, 052504.

(21) The oxygen was oriented at $+0.2223944$ bohr along the z-axis, the hydrogens were at $-0.8895776z$ and $\pm 1.4366479y$.

(22) Frisch, M. J.; Trucks, G. W.; Schlegel, H. B.; Scuseria, G. E..; Robb, M. A.; Cheeseman, J. R.; Montgomery, J. A., Jr.; Vreven, T.; Kudin, K. N.; Burant, J. C.; Millam, J. M.; Iyengar, S. S.; Tomasi, J. Barone, V.; Mennucci, B.; Cossi, M.; Scalmani, G.; Rega, N.; Persson, G. A.; Najatsuji, H.; Hada, M.; Ehara, M.; Toyota, K.; Fukuda, R.; Hasegawa, J.; Ishida, M.; Nakajima, T.; HOnda, Y.; Kitao, O.; Nakai, H.; Klene, M.; Li, X.; Knox, J. E.; Hratchian, H. P.; Cross, J. B.; Bakken, V.; Adama, C.; Jaramillo, J.; Gomperts, R.; Stratmann, R. E.; Yazyev, O.; Austin, A. J.; Cammi, R.; Pomelli, C.; Ochterski, J. W.; Ayala, P. Y.; Morokuma, K. Voth, G. A.; Salvador, P.; Dannenberg, J. J.; Zakrzewski, V. G.; Dapprich, S. Daniels, A. D.; Strain, M. C.; Farkas, O.; Malick, D. K.; Rabuck, A. D.; Raghavachari, K.; Foresman, J. B.; ORtiz, J. V.; Cui, Q.; Baboul, A. G.; Clifford, S.; Cioslowski, J.; Stefanov, B. B>; Liu, G.; Liashenko, A>; Piskorz, I.; Komaromi, I.; Martin, R. L.; Fox, D. J.; Keith, T.; Al-Laham, M. A.; Peny, C. Y.; Nanayakkara, A.; Challacombe, M.; Gill, P. M. W.; Johnson, B.; Chen, W.; Wong, M. W.; Gonzalez, C.; Pople, J. A. *Gaussian03*, revision C.02; Gaussian, Inc.: Wallingford, CT, 2004.

(23) Snatzke, G. *Angew. Chem., Int. Ed.* **1979**, *18*, 363−377.

(24) Jackson, S. M.; Nield, V. M.; Whitworth, R. W.; Oguro, M.; Wilson, C. C. *J. Phys. Chem. B* **1997**, *101*, 6142−6145.

(25) Fukazawa, H.; Hoshikawa, A.; Yamauchi, H.; Yamaguchi, Y.; Ishii, Y. *J. Cryst. Growth* **2005**, *282*, 251−259.

(26) McKinnnon, W. B.; Hofmeister, A. M. Proceedings of the 37th American Astronomical Society Division of Planetary Sciences Meeting, Sept 4−9, 2005; American Astronomical Society: Washington, DC, 2005.

(27) Fukazawa, H.; Hoshikawa, A.; Ishii, Y.; Chakoumakos, B. C.; Fernandez-Baca, J. A. *Astrophys. J*. **2006**, *652*, L57−L60.

(28) Kaminsky, W.; Claborn, K.; Kahr, B. *Chem. Soc. Rev*. **2004**, *33*, 514−525.